Characterization of thermo-mechanical behavior and adiabatic shear band formation in a press-hardened 22MnB5 steel at different strain rates

L. Schottstedt[1,*], M. Scholze[1], M. F.-X. Wagner[1]

[1] Institute of Materials Science and Engineering, Chemnitz University of Technology, Germany
*Corresponding author. Email: Luisa.Schottstedt@mb.tu-chemnitz.de

Abstract

Adiabatic Shear Band formation is observed in high-speed shear deformation of metallic materials, particularly in technologically relevant processes. It is characterized by the formation of increasingly localized areas of high shear strains. Depending on the selected process parameters, high-speed or adiabatic blanking can lead to the formation of an adiabatic shear band in the newly generated surface. These blanked surfaces have outstanding properties (e.g. high hardness, low rollover, low roughness, almost no burr) and can be used directly as functional surfaces. This reduces the need for complex and expensive, additional mechanical surface processing, significantly shortening the process chain and thus saving energy. In this contribution, we investigate the thermo-mechanical behavior and shear band formation of a press-hardened martensitic steel 22MnB5 under different strain rates. Tensile and compression tests are performed at different temperatures (in the range from 293 to 673 K) and in a wide range of nominal strain rates between 10^{-3} and $4 \cdot 10^{3}$ s^{-1}. In addition, we use S-shaped samples to introduce a simple shear stress state to generate (adiabatic) shear bands, again while applying quasi-static and dynamic (nominal) strain rates, respectively. The plane surface of this sample geometry enables an in-situ observation of local strain fields by digital image correlation. We show the mechanical similarities and differences of dynamic versus quasi-static shear experiments using digital image correlation. Our experimental approach contributes to a deeper understanding of the rate and stress-state dependent formation of shear bands in press-hardened steels.

Keywords

thermo-mechanical behavior, shear band, strain rate dependency, dynamic testing

1 Introduction

The production of metallic sheets with functional surfaces and customized properties usually requires several time-consuming processing steps. High-speed blanking is a promising technique for achieving specific mechanical and microstructural properties in the blanked surfaces while at the same time significantly reducing the number of subsequent machining steps (Schmitz et al., 2020). This includes a uniform surface quality, high hardness, almost no burr as well as higher dimensional accuracy. A key phenomenon observed in this process is the formation of adiabatic shear bands (ASBs), which significantly influences the final material properties, as the cut surfaces consist of separated shear bands. ASBs commonly occur in metallic materials subjected to high shear strain rates, particularly in titanium alloys (Scholze et al., 2025a), tantalum (Nesterenko et al., 1997) as well as high-strength steels (Roux et al., 2015). The underlying mechanisms and the temporal sequence of their evolution are still not fully understood. Several, to some extent contradictory, explanations are described in the literature, including (quasi-) adiabatic heating and thereby thermal softening (Zener and Hollomon, 1944), substantial temperature increases due to frictional heating at fracture surfaces (Goviazin and Rittel, 2023), as well as the role of dynamic recrystallization (DRX) in ASB evolution (Rittel et al., 2008; Rodríguez-Martínez et al., 2015). In particular, the contribution of microstructural mechanisms in shear band formation has not yet been fully resolved.

Martensitic steels, as key engineering materials, exhibit pronounced ASB formation under rapid shear loading conditions (Jo et al., 2020). While ASBs in these materials have traditionally been associated with negative effects, such as structural instabilities and uncontrolled failure (Dodd, 2012), they can also be utilized in high-speed blanking to reduce processing forces while enhancing the cutting quality of functional surfaces (Schmitz et al., 2020). A thorough understanding of the thermo-mechanical behavior associated with ASB formation plays an important role for optimizing material processing and precisely controlling the properties of the cut surfaces formed by ASBs.

In this study, we investigate the thermo-mechanical behavior of a press-hardened 22MnB5 steel over a wide range of temperatures (293 K to 673 K) and strain rates, from quasi-static to dynamic conditions. For an investigation of shear band formation, simple shear tests are performed using an S-shaped sample geometry under quasi-static and high-rate conditions, combined with digital image correlation (DIC) and subsequent microstructural analysis. The results form a basis for a deeper understanding of ASB formation, particularly in terms of correlations between uniaxial thermo-mechanical behavior, shear localization, and the resulting microstructures.

2 Materials and experiments

Sheets of commercially pure 22MnB5 (1.5528) steel with a thickness of 2 mm were obtained from Salzgitter Mannesmann Forschung GmbH (Salzgitter, Germany). The chemical composition was validated by glow discharge optical emission spectroscopy as 0.19 wt.% C, 1.04 wt.% Mn, 0.001 wt.-% B, 0.22 wt.% Si, 0.77 wt.% Cr and 0.21 wt.% Ni (with balance Fe). The material was first austenitized in a chamber furnace at 1203 K for 6 minutes and

then press-hardened using a water-cooled steel plate tool by Salzgitter Automotive Engineering GmbH & Co. KG (Osnabrück, Germany). To investigate the strain-rate and temperature dependence of the mechanical behavior of the press-hardened steel, uniaxial tensile and compression tests were conducted under various strain rates at room temperature and elevated temperatures (473 K and 673 K). Quasi-static and mid-range strain rate tests were performed at nominal strain rates of 10^{-3} s^{-1}, 1 s^{-1}, and 10 s^{-1} using tensile specimens (50 mm gauge length, 10 mm width) that were machined by laser cutting. The tests were carried out in a Schenck PTT 250 K1 (Carl Schenck AG, Darmstadt, Germany) hydraulic universal testing machine, equipped with a 250 kN load cell and a custom-built conductive heating system. To obtain thermo-mechanical data at high strain rates, dynamic compression tests of cylindrical specimens (2 mm diameter, 2 mm height, machined by electrical discharge machining) were performed with a nominal strain rate of $4 \cdot 10^3$ s^{-1} using a Split-Hopkinson Pressure Bar (SHPB) setup equipped with an inductive heating system. Strain measurements in all testing setups were performed using DIC. For tests at a nominal strain rate of 10^{-3} s^{-1}, an ARAMIS Adjustable 24M system from Carl Zeiss GOM Metrology GmbH (Braunschweig, Germany) was used. For mid-range to high strain rates, a high-speed camera (Fastcam SA5, Photron, Tokyo, Japan) was used to record the deformation. Conductive heating (for tensile tests) and inductive heating (for SHPB compression tests) were configured to ensure that the test temperature was reached prior to testing within a short time interval of 10 seconds in both cases, minimizing long-term thermal effects. Three samples were tested for each strain rate and temperature.

To specifically investigate ASB formation in press-hardened 22MnB5, S-shaped samples were machined from the 2 mm sheets using electrical discharge machining. The plane geometry of the shear sample, with an overlap length of 1.6 mm, was designed to result in a stress state that approaches simple shear during nominal uniaxial compressive loading of the sample while simultaneously allowing for DIC measurements (Scholze et al., 2025b). The S-shaped sample has a height of 13.4 mm and a width of 10 mm. The 1 mm notches are machined at an angle of 45°. For further details on notch root radii etc. the reader is referred to (Scholze et al., 2025b). Quasi-static shear testing (with a crosshead displacement rate of 0.0016 mm/s) was conducted in a ZwickRoell UPM1475 universal testing machine (ZwickRoell GmbH & Co. KG, Ulm, Germany), with the ARAMIS Adjustable 24M system used for in-plane deformation capturing. Similar to the compression tests, dynamic shear experiments were performed using the SHPB setup with a striker velocity of approximately 9 m/s. A Kirana ultra-high-speed camera (Specialised Imaging Ltd., Pitstone, United Kingdom) was used for in-plane recording of the deformation of the S-shaped samples during dynamic shear testing and to document ASB propagation. The DIC data was evaluated using the Zeiss Inspect Correlate 2023 software. Conventional metallographic preparation, including hot mounting, grinding, polishing, and etching (925 ml ethanol, 25 g picric acid, 50 ml hydrochloric acid), of the fractured samples was carried out. Optical microscopy was performed using an Olympus GX51 inverted reflected-light microscope (Olympus Corporation, Tokyo, Japan).

3 Results and discussion

In **Fig. 1** the engineering stress-strain curves from uniaxial mechanical testing of the 22MnB5 press-hardened steel at different strain rates and temperatures are shown. The results from testing at the highest rate, performed in the SHPB, exhibit some fluctuations that are associated with wave propagation effects. We observe that strength generally decreases with increasing temperature. This thermal softening phenomenon is more pronounced between 473 K to 673 K than from room temperature (293 K) to 473 K. Also, at elevated temperatures a decrease of ductility with increasing strain rate occurs; some experiments in the mid-range nominal strain rates at elevated temperatures were interrupted prematurely due to closed-loop feedback control issues in the challenging thermo-mechanical setup. During quasi-static testing at 673 K (Fig. 1a), an early onset of plastic instability is observed, which is directly related to thermal and microstructural softening mechanisms at elevated temperatures, as also observed in (Winter et al., 2017).

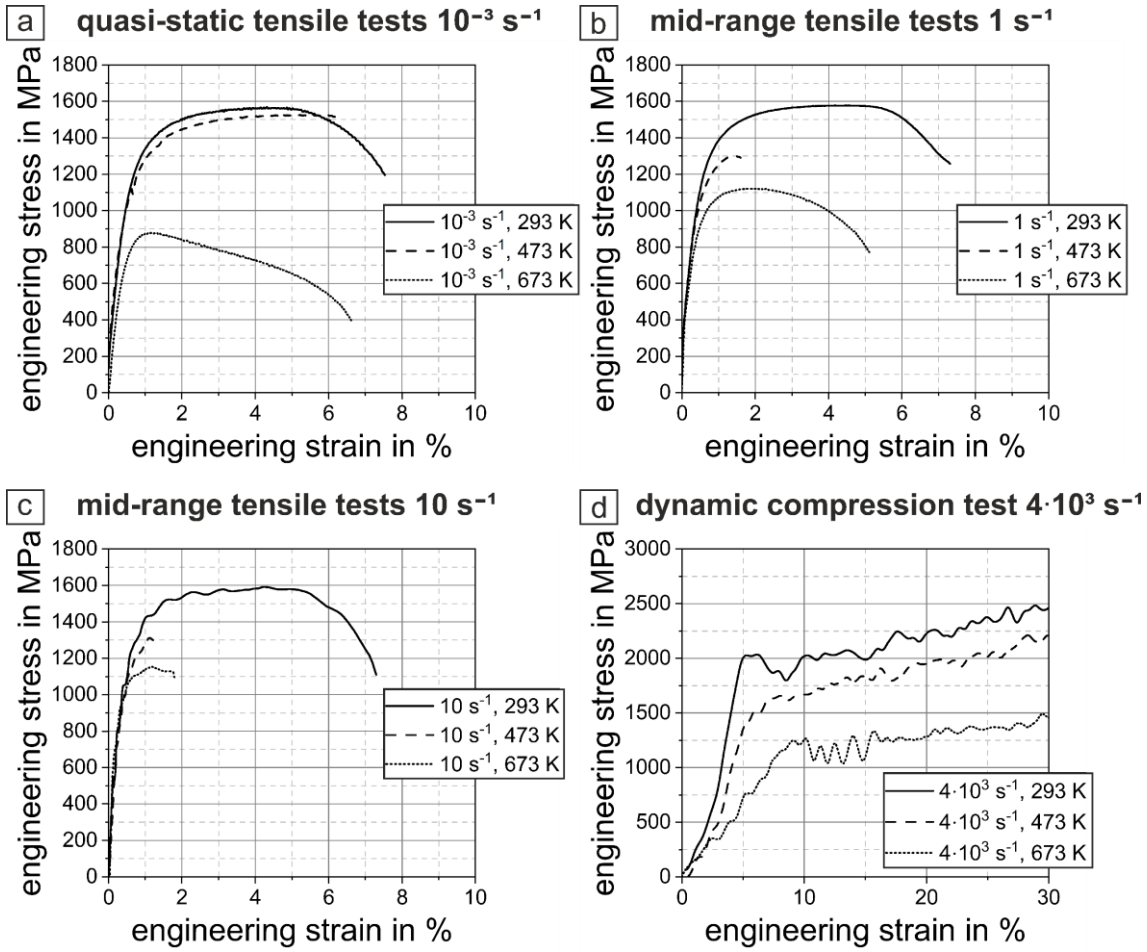

Figure 1: *Engineering stress-strain curves of representative samples deformed at 293 K, 473 K and 673 K, at strain rates of (a) 10^{-3} s^{-1}, (b) 1 s^{-1}, (c) 10 s^{-1} , and (d) $4{\cdot}10^{3}$ s^{-1}.*

Since the stress level for all three quasi-static to mid-range strain rates is almost identical at 293 K, the strain-rate sensitivity seems to be relatively low (which agrees with results

reported in (Schmitz et al., 2020)) in contrast to that at elevated temperatures. We note that, for a well-defined determination of the strain-rate sensitivity, it would be necessary to perform jump-tests to separate rate effects from those of microstructural evolution, which is most pronounced at elevated temperatures due to thermal effects and also depends on the duration of individual tests.

Strain hardening, thermal softening and strain rate hardening directly influence the formation and growth of ASBs. When thermal (or microstructural) softening overcomes the hardening terms, adiabatic shear banding can occur (Dodd, 2012). To investigate and generate (adiabatic) shear bands in the 22MnB5 sheet, we performed simple shear testing, both at quasi-static and dynamic nominal shear rates, until fracture of the samples. In **Fig. 2**, representative DIC fields of shear strain and shear strain rate for the simple shear tests are shown. For both nominal strain rates the DIC fields have been selected to represent the deformation stage just before fracture. The shear deformation zone is somewhat inclined with respect to the global loading direction in the case of quasi-static loading. Moreover, the local deformation is illustrated by thin black lines spanning the entire sample from top to bottom. The deformation of the samples, concentrated in the well-defined shear zone, results in an S-shape of these lines. Shear strain and shear strain rate are further evaluated along the central black line in the DIC fields. The corresponding line profiles are visualized in Figs. 2e and f. Clearly, the shear strain deformation zone is wider for quasi-static testing (with a width of about 400 µm) than the corresponding zone for dynamic shear testing (approx. 200 µm). The maximum shear strain before fracture is determined from the DIC data as 2.16 for the quasi-static and 0.94 for the dynamic case.

The shear strain rate data demonstrate the localized deformation mode inherent in S-shaped sample testing: shear strain rates are concentrated in the center of the shear zones, and the maximum, local shear strain rates 0.0346 s^{-1} for quasi-static and up to 320 000 s^{-1} for dynamic testing, respectively) exceed the nominal deformation rates by several orders of magnitude. These results demonstrate the effect of thermal softening on shear localization in the S-shaped samples, and they are also in line with our observations from uniaxial testing: under quasi-static shear loading, thermal effects (self-heating) hardly affect the mechanical response and strain hardening is the dominating mechanism. In contrast, under dynamic loading conditions, thermal softening exceeds the contribution of strain-rate hardening and clearly leads to local instability, shear localization and ASB formation.

The local shear strain rate values discussed here are of course limited by the different spatial resolutions of the different camera systems used for the quasi-static and dynamic tests, respectively. For dynamic testing in particular 14 pixels per facet are required for DIC correlation, resulting in a size of 100 µm for one DIC facet. This is ten times larger than the ASB width of about 10 µm previously reported in shear compression tests of a similar press-hardened steel (Schmitz et al., 2020). Consequently, while the shear strain rate values reported here confirm the trend of increased rates associated with localized deformation in a shear band, the actual values can be expected to be even higher.

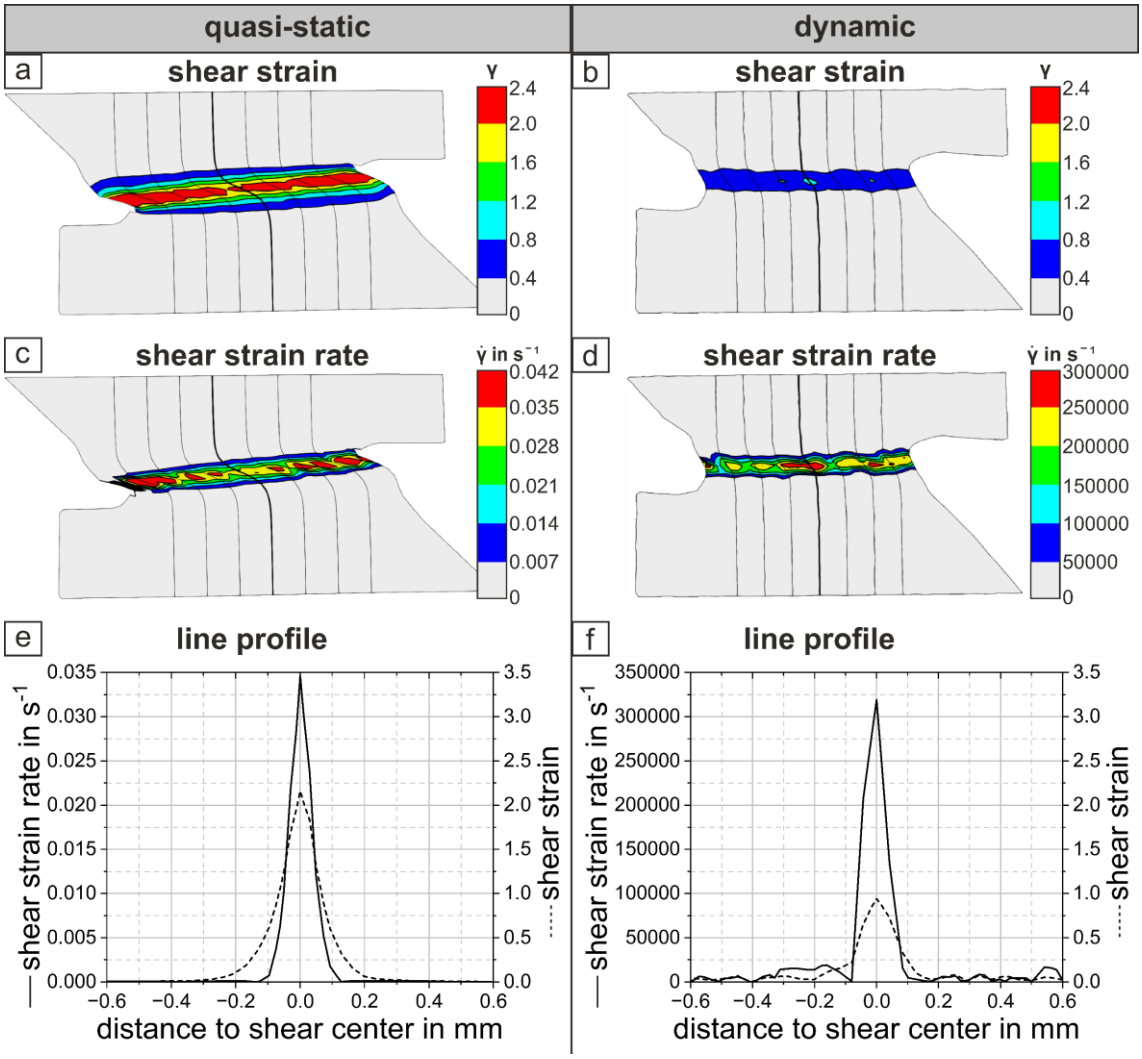

Figure 2: *Results of DIC measurements during quasi-static (10^{-3} s^{-1}) and dynamic ($4 \cdot 10^{3}$ s^{-1}) simple shear deformation. Distributions of (a) quasi-static shear strain, (b) dynamic shear strain, (c) quasi-static shear strain rate and (d) dynamic shear strain rate immediately before fracture. Lines from top to bottom indicate the local displacement fields. (e-f) Line profiles of shear strain and shear strain rate along the central black line.*

In **Fig. 3** optical micrographs taken from S-shaped simple shear samples (quasi-static and dynamically deformed until fracture) are shown. We observe a relatively wide deformation zone with a shear band half-width of at least 40 µm in the quasi-static sample (Fig. 3a) based on the strongly sheared martensitic microstructure. In contrast, the microstructure of the S-shaped sample deformed under dynamic loading condition (Fig. 3b) is characterized by an adiabatic shear band with a half-width of only approx. 4 µm and no noticeably deformed martensite in the vicinity. This clearly confirms that deformation and microstructural changes are strongly limited to a very narrow shear band region (that could be fully resolved by our DIC measurements) under dynamic loading conditions.

We note in closing that that the fracture surface of the dynamically deformed shear samples is much smoother than the quasi-statically obtained fracture surface. This morphology is

particularly promising with respect to the proposed use of ASB formation during high-speed blanking to produce functional surfaces.

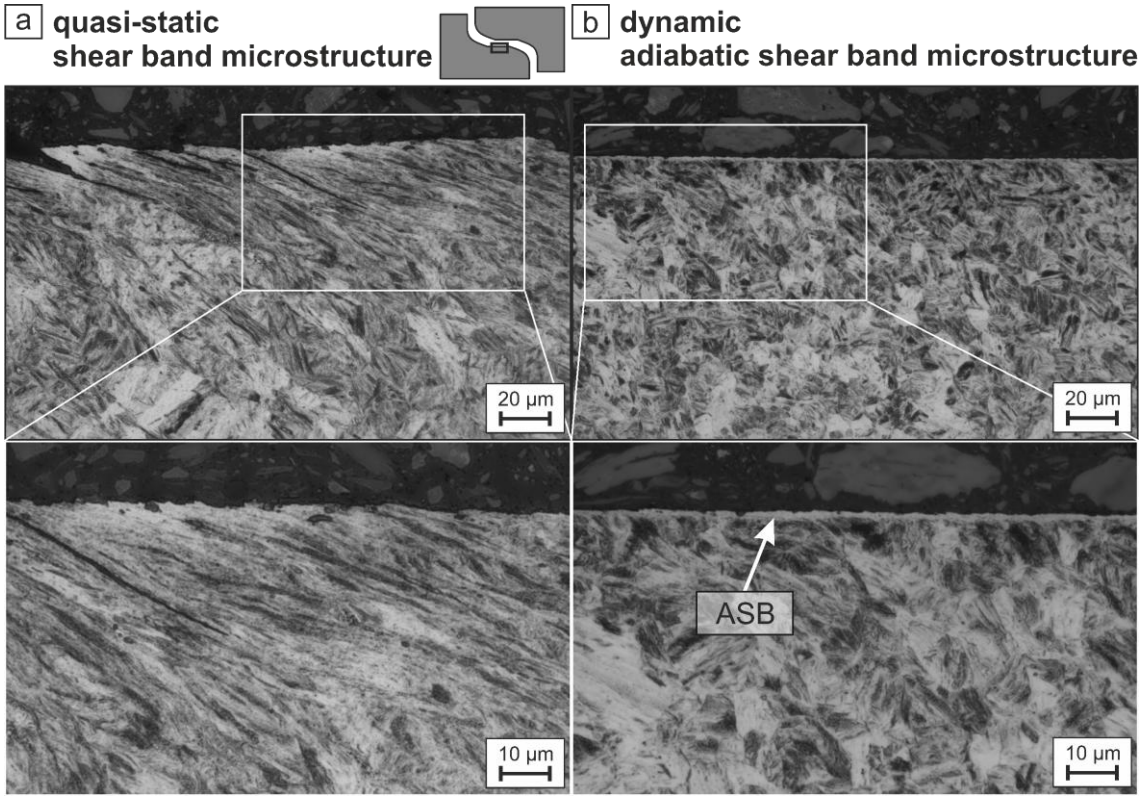

Figure 3: *Optical micrographs of (a) quasi-static and (b) dynamically deformed simple shear samples.*

4 Summary and conclusions

In summary, we investigated a press-hardened 22MnB5 steel by characterizing the thermo-mechanical behavior under different strain rates (10^{-4} to $4 \cdot 10^{3}$ s^{-1}) and temperatures (293 to 673 K) using uniaxial tensile and compression tests. We then used S-shaped samples to introduce a simple shear stress state while applying quasi-static and dynamic (nominal) strain rates. The key results can be summarized as follows:

- Thermal softening: Strength decreases significantly between 293 K, 473 K and 673 K, with a ductility reduction at elevated strain rates.
- Strain-rate sensitivity: Low positive strain-rate sensitivity at 293 K and higher strain rate-sensitivity values at elevated temperatures.
- Quasi-static simple shear: Shear strain width of approx. 400 µm, maximum shear strain of 2.16 and maximum shear strain rate of 0.0346 s^{-1} determined by DIC. Shear band half-width: 40 µm.
- Dynamic simple shear: Shear strain width of approx. 200 µm, maximum shear strain of 0.94 and maximum shear strain rate of 320 000 s^{-1}. Local shear strain rates are presumably higher than calculated from DIC data due to the spatial resolution of the high-speed camera.

- Microstructural evidence for distinct shear localization under dynamic loading conditions is given in the investigated ASB with a shear band half-width of 4 µm.

Acknowledgments

This work was supported by the German Research Foundation (Deutsche Forschungsgemeinschaft DFG) within the Research Unit FOR 5380 “Functional surfaces through adiabatic high-speed processes: Microstructure, mechanisms and model development - FUNDAM^{3}ENT” (grant number 460484491). The authors would like to thank Felix Schubert and Christoph Wollschläger for their contributions to the mechanical testing.

References

Dodd, B., 2012. Adiabatic shear localization: Frontiers and advances, 2. ed. ed. Elsevier, Amsterdam, Heidelberg, 454 pp.

Goviazin, G.G., Rittel, D., 2023. *Revisiting the hot adiabatic shear band paradigm*. International Journal of Impact Engineering 180, 104702.

Jo, M.C., Kim, S., Suh, D.W., Hong, S.S., Kim, H.K., Sohn, S.S., Lee, S., 2020. *Effect of tempering conditions on adiabatic shear banding during dynamic compression and ballistic impact tests of ultra-high-strength armor steel*. Materials Science and Engineering: A 792, 139818.

Nesterenko, V.F., Meyers, M.A., LaSalvia, J.C., Bondar, M.P., Chen, Y.J., Lukyanov, Y.L., 1997. *Shear localization and recrystallization in high-strain, high-strain-rate deformation of tantalum*. Materials Science and Engineering: A 229 (1-2), 23–41.

Rittel, D., Landau, P., Venkert, A., 2008. *Dynamic recrystallization as a potential cause for adiabatic shear failure*. Physical review letters 101 (16), 165501.

Rodríguez-Martínez, J.A., Vadillo, G., Rittel, D., Zaera, R., Fernández-Sáez, J., 2015. *Dynamic recrystallization and adiabatic shear localization*. Mechanics of Materials 81, 41–55.

Roux, E., Longère, P., Cherrier, O., Millot, T., Capdeville, D., Petit, J., 2015. *Analysis of ASB assisted failure in a high strength steel under high loading rate*. Materials & Design 75, 149–159.

Schmitz, F., Winter, S., Clausmeyer, T., Wagner, M.F.-X., Tekkaya, A., 2020. *Adiabatic blanking of advanced high-strength steels*. CIRP Annals 69 (1), 269–272.

Scholze, M., Winter, S., Frint, P., Böhme, M., Wagner, M.F.-X., 2025a. *Morphology of adiabatic shear bands in a metastable beta titanium alloy depends on initial microstructure*. Materials Science and Engineering: A 924, 147832.

Scholze, M., Schottstedt, L., Hinze, M., Frint, P., Wagner, M.F.-X., 2025b. *Tailored planar S-shaped samples for in-situ characterization of adiabatic shear banding under controlled stress triaxialities*. International Journal of Impact Engineering.

Winter, S., Schmitz, F., Clausmeyer, T., Tekkaya, A.E., Wagner, M.F.-X., 2017. *High temperature and dynamic testing of AHSS for an analytical description of the adiabatic cutting process*. IOP Conference Series: Materials Science and Engineering 181, 12026.

Zener, C., Hollomon, J.H., 1944. *Effect of Strain Rate Upon Plastic Flow of Steel*. Journal of Applied Physics 15 (1), 22–32.